Covalent Adduct Formation in Methylthio-D-ribose-1-Phosphate Isomerase: Reaction Intermediate or Artifact?

Journal:	*Biochemistry*
Manuscript ID	bi-2022-00142e.R1
Manuscript Type:	Article
Date Submitted by the Author:	n/a
Complete List of Authors:	Veeramachineni, Vamsee; University at Buffalo - The State University of New York, Chemistry Ubayawardhana, Subashi; University at Buffalo - The State University of New York, Chemistry Murkin, Andrew; University at Buffalo - The State University of New York, Chemistry

Covalent Adduct Formation in Methylthio-D-ribose-1-Phosphate Isomerase: Reaction Intermediate or Artifact?

Vamsee M. Veeramachineni,† Subashi T. Ubayawardhana, and Andrew S. Murkin*

Department of Chemistry, University at Buffalo, The State University of New York, Buffalo, New York, 14260-3000, United States

ABSTRACT: Methylthio-D-ribose-1-phosphate (MTR1P) isomerase (MtnA) functions in the methionine salvage pathway by converting the cyclic aldose MTR1P to its open-chain ketose isomer methylthio-D-ribulose 1-phosphate (MTRu1P). What is particularly challenging for this enzyme is that the substrate's phosphate ester prevents facile equilibration to an aldehyde, which in other aldose–ketose isomerases is known to activate the α-hydrogen for proton or hydride transfer between adjacent carbons. We speculated that MtnA could use covalent catalysis via a phosphorylated residue to permit isomerization by one of the canonical mechanisms, followed by phosphoryl transfer back to form the product. In apparent support of this mechanism, [^{32}P]MTR1P was found by SDS-PAGE and gel-filtration chromatography to radiolabel the enzyme. Susceptibility of this adduct to strongly acidic and basic pH and nucleophilic agents is consistent with an acyl phosphate. C160S and D240N, mutants of two conserved active-site residues, however, exhibited no difference in radiolabeling despite a reduction in activity of ~10^7, leading to the conclusion that phosphorylation is unrelated to catalysis. Unexpectedly, prolonged incubations with C160S revealed up to 30% accumulation of radioactivity, which was identified by ^{31}P and ^{13}C NMR to be the result of a second adduct—a hemiketal formed between Ser160 and the carbonyl of MTRu1P. These results are interpreted as indirect support for a mechanism involving transfer of the proton from C-2 to C-1 by Cys160.

Introduction

Reduced forms of sulfur, such as the thiol and sulfide groups of the amino acids cysteine and methionine, are valuable biological commodities because their production from natural inorganic sources is energetically demanding.[1-4] One of the most useful derivatives of methionine, *S*-adenosylmethionine, serves in several capacities, including alkylation of a wide array of biomolecules via the transfer of its methyl, adenosyl, or — following decarboxylation — aminopropyl group. This last function serves in the synthesis of the polyamines spermine and spermidine, resulting in the formation of 5′-methylthioadenosine (MTA) as a byproduct. In order to reclaim the sulfide group in MTA, it is recycled back to methionine and SAM by the action of the methionine salvage pathway (Scheme 1). Although the presence of this pathway in organisms as diverse as bacteria, yeast, mammals, and plants was verified long ago, the study of the responsible enzymes and their catalytic mechanisms is still not complete. Of particular interest is the mechanism involved in the aldose–ketose isomerization of 5-methylthio-D-ribose 1-phosphate (MTR1P) to 5-methylthio-D-ribulose 1-phosphate (MTRu1P) catalyzed by MTR1P isomerase (MtnA).[5]

In general, aldose–ketose isomerases utilize one of two canonical mechanisms that require the existence of a carbonyl group in the substrate or a form with which it is in equilibrium:[6,7] (1) proton transfer and (2) hydride transfer (Scheme 2). Exemplified by triose phosphate isomerase,[8,9] ribose-5-phosphate isomerase, glucose-6-phosphate isomerase,[10] and mannose-6-phosphate isomerase, the proton-transfer mechanism is the more common of the two mechanisms. A single Brønsted base relays the α-proton between two adjacent carbon atoms via a *cis*-enediol(ate) intermediate, and this process usually results in partial exchange of the proton with the solvent. In the case of the hydride-transfer mechanism, isomerization proceeds through a 1,2-hydride shift in an activated substrate. The

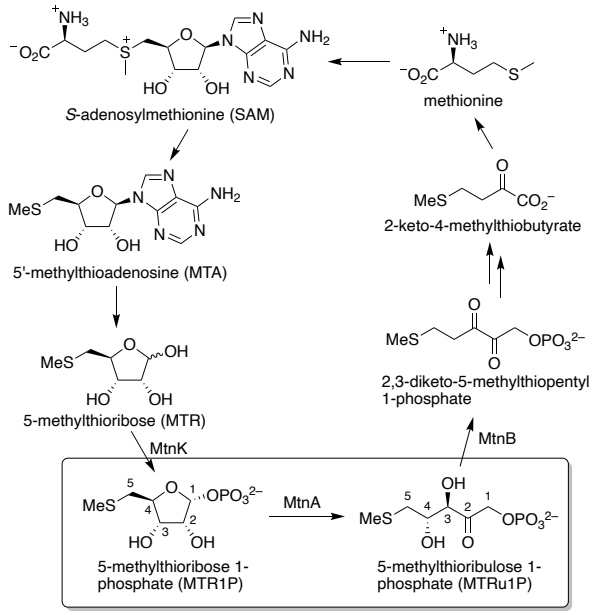

Scheme 1. The methionine salvage pathway of *Bacillus subtilis*, featuring methylthioribose-1-phosphate (MTR1P) isomerase (MtnA). MtnK, methylthioribose (MTR) kinase; MtnB, methylthioribulose-1-phosphate (MTRu1P) dehydratase.

activation involves formation of an alkoxide ion by the removal of an alcoholic proton. Although hydride transfer is favored in the presence of a specific base,[11] enzymes using this mechanism are known to use a divalent metal ion that is coordinated by the carbonyl group and the α-hydroxyl, thereby lowering its pK_a while also polarizing the carbonyl group by induction. Enzymes using this mechanism, such

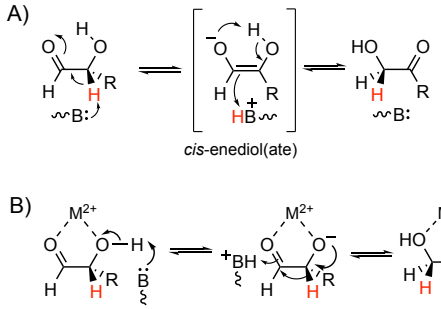

Scheme 2. Canonical mechanisms of enzyme-catalyzed aldose–ketose isomerization. A) Proton-transfer mechanism, B) hydride-transfer mechanism.

as xylose isomerase,[12] show little or no exchange of label with the solvent.[13]

What makes the MtnA-catalyzed reaction especially interesting is that the presence of the phosphate ester in its aldose substrate MTR1P precludes equilibration to an aldehyde, and therefore, MtnA cannot utilize one of the canonical mechanisms. Observations from previous investigations have revealed some hints at MtnA's mechanism. When the reaction was conducted in D_2O, no deuterium was incorporated into the product, a result that favors transfer of a hydride;[14] however, this is at odds with the lack of a divalent metal ion in MtnA and can alternatively be explained by a mechanism in which the transferred proton is sequestered from bulk solvent. Using [1-^{2}H]- and [2-^{2}H]ribose 1-phosphate as the substrate, Imker et al. demonstrated that H-2 is transferred suprafacially between C-1 and C-2.[15] Tamura et al. subsequently published the crystal structure of the *Bacillus subtilis* MtnA–product complex, prompting them to propose two mechanisms consistent with the stereospecific hydrogen transfer.[16] As shown in Scheme 3A, protonation of the

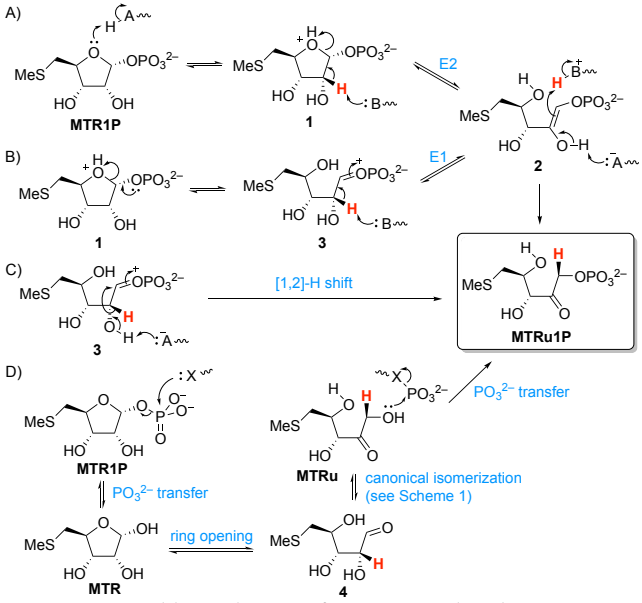

Scheme 3. Possible mechanisms for MtnA-catalyzed isomerization of MTR1P to MTRu1P.

ring oxygen was assumed to occur first in order to weaken the C1–O4 bond and to introduce a neutral leaving group. From **1**, concerted deprotonation at C-2 and ring opening would produce *cis*-enediol intermediate **2** (i.e., E2 elimination). Tautomerization involving transfer of the same proton back to C-1 without solvent exchange yields MTRu1P. Alternatively, ring opening of **1** to produce oxocarbenium ion **3** (i.e., E1 elimination, Scheme 3B) could occur prior to deprotonation at C-2, although the authors did not mention this stepwise possibility. Note that **3** is stabilized by resonance and induction from the neighboring dianionic phosphate. Instead of deprotonation of **3**, the second mechanism they suggested involves deprotonation at O-2 in concert with a [1,2]-hydride shift (Scheme 3C).

What has not yet been considered is a mechanism involving phosphoryl transfer to an enzymatic nucleophile (Scheme 3D). This process may occur with protonation at O-1 to yield methylthioribose (MTR) as an intermediate, which would subsequently ring open to aldehyde **4**; alternatively, if O-4 is protonated instead, phosphoryl transfer may occur in concert with ring opening (not shown). In either case, **4** would be subject to one of the canonical mechanisms described in Scheme 2, followed by phosphoryl transfer back to methylthioribulose (MTRu) to yield MTRu1P. Studying the fate of the phosphate group may therefore clarify the mechanism of MtnA-catalyzed isomerization.

The unique nature of the chemistry along with the enigmatic discovery that the human orthologue doubles as a mediator of RhoA-dependent cell invasion associated with melanoma makes MtnA interesting to study.[17] In this article, we describe two covalent adducts observed by radioactive labeling and evaluate their catalytic relevance in light of the newly suggested covalent mechanism.

Experimental Procedures

Expression and Purification of Methionine Salvage Pathway Enzymes. pET15b plasmids containing the genes encoding N-terminal His_6-tagged *B. subtilis* MtnK, MtnA, and MtnB were obtained from Prof. John Gerlt (University of Illinois).[15] *Escherichia coli* BL21(DE3) cells were transformed by introduction of the plasmids, and the bacterial cultures were prepared by transferring 10 mL of overnight starter culture into 1 L of sterile LB-Miller broth containing 100 mg/L ampicillin. Cultures expressing MtnK and MtnB were shaken for 36 h at 37 °C, while those expressing MtnA were cooled down to 25 °C after reaching an OD_{600} of 0.6, followed by protein induction overnight using 0.5 mM IPTG. The cells were harvested by centrifugation at 5000 rpm, and the pellet was resuspended in a 20 mM Tris-HCl (pH 7.9) containing 5 mM $MgCl_2$, cOmplete protease inhibitor cocktail (Roche Diagnostics) and 5–10 mg DNase I. The cells were then ruptured using a M-110L Microfluidizer processor (Microfluidics), followed by centrifugation at 13,000*g* to remove the cell debris. The supernatant was passed through a 45-μm syringe filter (Corning) and applied to a Ni^{2+}-charged HisPrep FF 16/10 column (GE Healthcare; column volume, CV = 20 mL) that was previously equilibrated with Buffer A (50 mM Tris-HCl, 500 mM NaCl and 5 mM $MgCl_2$, pH 7.8). After loading the protein, the column was washed with five CV (100 mL) of 5% Buffer B (Buffer A plus 500 mM imidazole, pH 7.8) in Buffer A. The protein was eluted with a linear 5–100% gradient against Buffer B over nine CV using an ÄKTA Explorer 10 FPLC system (GE Healthcare). Fractions were evaluated using SDS-PAGE under reducing conditions, and fractions containing the protein were pooled and concentrated with an Amicon ultrafiltration device (10 kDa MWCO membrane). The concentrated protein was dialyzed against dialysis buffer (50 mM Tris, 100 mM NaCl, pH 7.8), flash-frozen in liquid nitrogen, and stored at −80 °C. Protein concentrations were determined spectrophotometrically using the extinction coefficient calculated from its amino acid sequence using the ProtParam utility:[18] MtnA, ε_{280} = 26,930 M^{-1} cm^{-1}; MtnB, ε_{280} = 27,960 M^{-1} cm^{-1}; MtnK, ε_{280} = 39,880 M^{-1} cm^{-1}.

Site-Directed Mutagenesis. Mutants of MtnA were constructed using the QuikChange Site-Directed Mutagenesis Kit (Agilent) according to the manufacturer's instructions. Primer sequences were as follows: C160S, 5′-ATTGAGCCGGCATTGCTGATCGTCATGATCCTG-3′ (forward) and 5′-CAGGATCATGACGATCAGCAATGCCGGCTCAAT-3′ (reverse); D240N, 5′-GTTCTTTGCAATTCGGTTGGCTCCGACGATAACAG-3′ (forward) and 5′-CTGTTATCGTCGGAGCCAACCGAATTGCAAAGAAC-3′ (reverse). A pET15b plasmid encoding C160A was purchased from GenScript USA, Inc. The presence of mutations was verified by DNA sequencing, and the proteins were expressed (50 μM IPTG for C160A and 500 μM for all others) and purified as described for the wild-type enzyme.

Synthesis of Methylthio-D-ribose (MTR), [2-^{2}H]-, [1-^{13}C]-, [2-^{13}C]-, and [1,2-$^{13}C_2$]MTR. Unlabeled MTR was synthesized from methyl 2,3-*O*-isopropylidene-β-D-ribofuranoside[19] (Combi-Blocks. Inc.) by tosylation or triflation, substitution with excess sodium thiomethoxide, and acid-catalyzed deprotection according to literature.[20] [2-^{2}H]-, [1-^{13}C]-, [2-^{13}C]-, and [1,2-$^{13}C_2$]MTR were synthesized by the same procedure after first converting the correspondingly labeled D-ribose (Omicron Biochemicals, Inc.) to the 2,3-*O*-isopropylidene-protected methyl glycoside according to the literature procedure.[19] The final yield of unlabeled and labeled MTR was 65–75%.

Enzymatic Synthesis and Purification of MTR1P, [2-^{2}H]-, [1-^{13}C]-, [2-^{13}C]-, and [1,2-$^{13}C_2$]MTR1P. Unlabeled MTR1P was synthesized from MTR using MtnK and ATP as follows. A typical reaction (10 mL) contained 40 mM MTR, 45 mM ATP, 5 mM $MgCl_2$, 5 mM DTT, 20 mM Tris-HCl (pH 7.9) and 5 μM MtnK. The reaction progress at 37 °C was monitored by the decrease in pH, which was adjusted occasionally with 0.1 M KOH. At completion, as indicated by the OPDA assay (see below), the pH was reduced to 4 using 0.1 M HCl to precipitate the protein. After centrifugation, the supernatant was filtered through a bed of charcoal (2 g) over diatomaceous earth, which was washed with 100 mL of 5% aqueous ethanol. The filtrate was concentrated and applied to an anion exchange column (1.5 cm × 20 cm, Amberlite IRA 400, HCO_3^- form), eluting with an increasing step gradient of triethylammonium bicarbonate (TEAB): 250 mL of 50 mM, 250 mL of 100 mM, 2 L of 200 mM, and 500 mL of 500 mM. MTR1P was identified in the 200 mM fraction, which was evaporated to dryness multiple times. To remove remaining TEAB, the resulting solid was dissolved in water and passed through a RediSep Rf Gold reversed-phase C18 column (15.5 g, CV = 13.5 mL) and was eluted with 50% aqueous methanol. Fractions containing MTR1P were identified by the malachite green assay (see below). Pooled fractions were converted to the sodium salt by treatment with cation exchange resin (Amberlite IR 120 resin, Na^+ form).

[2-^{2}H]-, [1-^{13}C]-, [2-^{13}C]-, and [1,2-$^{13}C_2$]MTR1P were also enzymatically synthesized as described above, but the purification was altered for the smaller scale. After the acid precipitation step, the supernatant was filtered through diatomaceous earth without charcoal. The filtrate was evaporated to dryness and redissolved in 2 mL of 100 mM TEAB. Purification was achieved by reversed-phase HPLC on a semi-preparative column (Phenomenex Luna 5 μm C18(2), 250 × 21.2 mm), equilibrated with 97% solvent A (100 mM TEAB) and 3% solvent B (50% v/v aqueous methanol). A gradient program was applied as follows: 0–30 min, isocratic 3% B; 30–40 min, linear 3–20% B; 40–50 min, linear 20–50% B; 50–60 min, linear 50–100% B; hold at 100% A. Fractions were collected at an interval of 1 min at 8 mL/min. Those containing labeled MTR1P (typically 15–28) were pooled and evaporated to dryness multiple times from water to remove excess TEAB. Finally, cation exchange to the sodium salt was performed as described for unlabeled MTR1P.

Synthesis and Purification of [^{32}P]MTR1P. In a total volume of 1 mL, 100 μM MTR, 500–750 μCi [γ-^{32}P]ATP (PerkinElmer; sp. act. 3000 Ci/mmol), 5 mM $MgCl_2$, 5 mM DTT, and 20 mM Tris-HCl (pH 7.9) were mixed. Reaction was initiated by the addition of 10 μM MtnK, and the solution was allowed to react for 30 min at 37 °C. Unlabeled ATP (200 μM final) was then added and left to incubate for 90 min to drive the reaction to completion. The protein was removed by ultrafiltration (modified PES, 10 kDa cutoff), and labeled MTR1P was purified by reversed-phase HPLC on an analytical column (Waters Delta-Pak C18, 15 μm, 100 Å, 3.9 × 300 mm). Purification was performed at 2 mL/min using the following gradient protocol: 0–9 min, 100% A; 9–18 min, 0–5% B; 18–22 min, 5–50% B; 22–24 min, 50% B; 24–30 min, 100% A. Fractions containing [^{32}P]MTR1P were pooled, evaporated to dryness under reduced pressure, and quantified.

Detection and Quantification of MTR1P. For qualitative assay of MTR1P during purification (see above), the method of Baykov et al. using malachite green and ammonium molybdate with detection at 630 nm was employed.[21] Although this assay can be conducted quantitatively using a standard curve, MTR1P was quantified more conveniently by the *o*-phenylenediamine (OPDA) assay as follows.[5] Assay mixtures (1 mL) incubated at 25 °C contained 50 mM triethanolamine hydrochloride (TEOA-HCl) buffer (pH 7.5), 5 mM $MgCl_2$, 5 mM DTT, 20 mM OPDA, 10 μM MtnB, and MTR1P. Reactions were initiated by adding 100 nM MtnA. The concentration of the quinazoline product was calculated by the net absorbance change at 320 nm using $\varepsilon_{320} = 7.53 \pm 0.12$ mM^{-1} cm^{-1}, which was determined from the slope of a standard curve of absorbance change vs. MTR1P concentration. The MTR1P standard concentration in turn had been determined by ^{1}H-NMR spectroscopy by integration of its methyl singlet using imidazole as an internal standard, as described previously.[22]

Steady-State Kinetics. The OPDA assay described above was used in all kinetics measurements. Initial velocities were measured with MTR1P (20–800 μM) using 10 nM MtnA to initiate the reactions. These rates were corrected for background by subtracting the velocity obtained in the absence of the substrate. Initial velocities (v_o) normalized for the total concentration of MtnA ($[E]_t$) were fit to eq 1 by nonlinear regression using KaleidaGraph (Synergy Software) to determine the k_{cat} (left form), k_{cat}/K_M (right form), and K_M.

$$\frac{v_o}{[E]_t} = \frac{k_{cat}[S]}{[S]+K_M} = \frac{(k_{cat}/K_M)[S]}{[S]/K_M+1} \quad (1)$$

The pH dependence of MtnA activity was measured at pH 6.5–9.5 using the OPDA assay, employing a binary buffer system containing PIPES and TAPS (slight differences were observed when using each buffer individually). The concentration of MtnA was adjusted as needed, and initial velocities were normalized accordingly. Rates were verified to be independent of MtnB at all pH. k_{cat} and k_{cat}/K_M were calculated at each pH using eq 1 and plotted separately as a function of pH. Each profile was fit to eq 2 by nonlinear regression

$$k = c/(1 + 10^{pK_1-pH} + 10^{pH-pK_2}) \quad (2)$$

where k is the observed rate constant, c is its pH-independent limit, and K_1 and K_2 are the acid dissociation constants at low and high pH, respectively.

Primary Deuterium Kinetic Isotope Effects. The OPDA assay was repeated with both MTR1P and [2-^{2}H]MTR1P. Primary deuterium KIEs were calculated by analytical nonlinear regression using SigmaPlot (v. 12.5, Systat Software) by global fitting of steady-state data to eq 3

$$\frac{v_o}{[E]_t} = \frac{k_{cat}[S]}{K_M(1+F_iE_{V/K})+[S](1+F_iE_V)} \quad (3)$$

where $E_{V/K}$ and E_V are the isotope effects minus 1 on k_{cat}/K_M and k_{cat}, respectively, and F_i is the fraction of deuterium (i.e., 0 for MTR1P and 1 for [2-^{2}H]MTR1P).[23]

Electrophoresis of Radioactively Labeled Protein. MtnA (39–44 μM) and [^{32}P]MTR1P (80–91 μM) were incubated (1:2 mole ratio) in 20 mM TEOA·HCl (pH 7.8) for 30 s before quenching with a final concentration of 2% (w/v) sodium dodecyl sulfate (SDS). Non-reducing SDS-PAGE of 5 μL aliquots was performed on Mini PROTEAN TGX precast gels (Bio-Rad) in Tris–glycine buffer (0.1% SDS) at 50 V for 15 min followed by 100 V for 90 min. The protein was electroblotted onto a double-layer of PVDF membrane (Sequi-Blot PVDF Membrane, Bio-Rad), which was exposed to a phosphor screen (Molecular Dynamics) for 24 h before scanning on a phosphorimager (PharosFX Plus Molecular Imager, Bio-Rad). The PVDF membrane was then stained with an aqueous solution containing 0.1% Coomassie blue (Brilliant Blue R, Acros), 50% methanol, and 1% acetic acid for 30 s before destaining in three portions of 40% aqueous methanol for 5 min each.

Size-Exclusion Chromatography of Radioactively Labeled Protein. MtnA and [^{32}P]MTR1P were mixed as described above except with protein in excess over substrate to maximize the yield of radioactively labeled protein. Size exclusion chromatography was performed in a cold room (~6 °C) by syringe injection onto three 5-mL HiTrap desalting columns (GE Healthcare) connected in series. The columns were equilibrated and eluted using 20 mM NH_4HCO_3 (pH 7.8). Fractions (500 μL) were collected and analyzed for the presence of protein (absorbance at 280 nm) and ^{32}P signal (scintillation counting). The fractions containing radioactively labeled protein were pooled, frozen in liquid nitrogen, and stored at −80 °C for future use.

Effect of pH on Radioactively Labeled Protein. Multiple replicate samples of the 1:2 MtnA–[^{32}P]MTR1P reaction mixture were electrophoresed and transferred to PVDF membrane and stained with Coomassie, as described earlier. The lanes on the membrane were cut into separate strips and incubated for 30 min at 25 °C in 0.1 M buffer solutions varying in their pH as follows: pH 1, HCl/KCl; pH 3 and 5, citric acid–sodium citrate; pH 7, KH_2PO_4–K_2HPO_4; pH 9, $Na_2B_4O_7$/HCl; pH 11, $KHCO_3$/K_2CO_3. Unbuffered solutions at pH 13 and 14 were prepared from 1.0 M KOH. The strips were then reassembled and exposed to a phosphor screen for 24 h before scanning on a phosphorimager.

Enzyme samples purified by size exclusion chromatography were diluted 20-fold with each of the above buffers, incubated for 30 min at 25 °C, and passed through centrifugal filters (VWR Centrifugal Filters, Modified PES, 10 kDa MWCO, 500 μL) to remove the protein. A control sample was prepared using 20 mM NH_4HCO_3 (pH 7.8) followed immediately by ultrafiltration. The radioactivity of the filtrate was counted to determine the fraction of radioactively labeled protein adduct that remained intact.

Effect of Nucleophilic Agents on Radioactively Labeled Protein. Different concentrations of β-mercaptoethanol (BME), dithiothreitol (DTT), and tris(2-carboxyethyl)phosphine (TCEP) were prepared in Laemmli buffer. These buffers were incubated with the isomerase reaction before loading onto SDS-PAGE gels. After electrophoresis and electroblotting, the PVDF membranes were exposed to a phosphor screen and scanned on a phosphorimager.

Stock solutions (2X concentration) of NH_2OH and pyridine, prepared in 0.1 N Tris acetate buffer (pH 7), were incubated with equal volume of purified (SEC) radioactively labeled protein for required period at 25 °C. Nine volumes of tert-butyl alcohol were added followed by centrifugation at 13000 rpm at 4 °C to precipitate the protein. The liquid was decanted, protein pellet was washed with tert-butyl alcohol and counted in a scintillation counter after dissolving the protein pellet in 1% SDS solution. Controls were performed using BSA mixed with [^{32}P]MTR1P to confirm precipitation of only the protein and the radioactivity associated with the protein.

^{31}P- and ^{13}C-NMR Experiments. Equilibrated mixtures of unlabeled (for ^{31}P NMR) and 1-^{13}C-, 2-^{13}C-, and 1,2-$^{13}C_2$-labeled (for ^{13}C NMR) MTR1P and MTRu1P were prepared by incubating 4 mM appropriately labeled MTR1P with 2 μM wild-type MtnA in 20 mM TEOA buffer (pH 7.9). The mixture was subjected to ultrafiltration (10 kDa MWCO) to remove the wild-type enzyme, and the filtrate was incubated with 1.2 mM C160S for 1 h. The protein adduct was isolated using a HiTrap desalting column with 25 mM TEOA (pH 7.9) as the eluting buffer.

For ^{31}P NMR, the resulting unlabeled sample was analyzed on a Varian INOVA 500 spectrometer operating at 202.32 MHz, equipped with a broadband nanoprobe. A default pulse sequence for ^{31}P NMR with a 45° pulse, an acquisition time of 1 s, a relaxation delay of 1 s, and a spectral width of 10,105 Hz (from −35 to 20 ppm) were employed to acquire 4096 transients. An exponential line broadening function of 20 Hz was applied to each free-induction decay followed by a baseline correction for each transformed spectrum. For ^{13}C NMR, the resulting ^{13}C-labeled sample was analyzed on a Varian INOVA 300 spectrometer operating at 75 MHz, equipped with a broadband probe. A default pulse sequence for ^{13}C NMR with a 90° pulse, an acquisition time of 0.868 s, a relaxation delay of 1 s each, and a spectral width of 18867.9 Hz (from −15 to 235 ppm) were employed to acquire spectra overnight. An exponential line broadening function of 5 Hz was applied to each free-induction decay followed by a baseline correction for each transformed spectrum.

Results and Discussion

Steady-state Kinetics and pH Dependence. Steady-state kinetics measurements were made spectrophotometrically by coupling the product with the dehydratase (MtnB) and *o*-phenylenediamine (OPDA) (Scheme 4). k_{cat} and K_M were determined to be 2.5 s^{-1} and 124 μM, respectively, at pH 7.8 and 25 °C. This K_M is close to the previously reported value of 138 μM measured at 37 °C, but k_{cat} is over four times less than the value of 13 s^{-1}, likely owing to the higher temperature used in that study.[14]

To assess the importance of acid–base chemistry on catalysis, pH–rate profiles were constructed for k_{cat} and k_{cat}/K_M (Figure 1). Due to precipitation of MtnB at pH < 6.5, this was chosen as the low end of the pH range (6.5–9.5). Both graphs appear as bell-shaped curves with maximal values at pH 7.5–8.0. The pK_a associated with the basic limb is slightly higher for k_{cat} (8.9 ± 0.1) than for k_{cat}/K_M

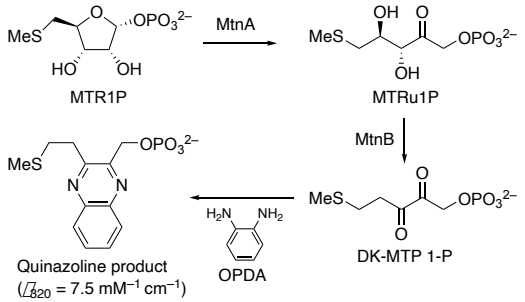

Scheme 4. Coupled assay for MtnA. DK-MTP 1-P, 2,3-diketo-5-methylthiopentyl 1-phosphate; OPDA, *o*-phenylenediamine.

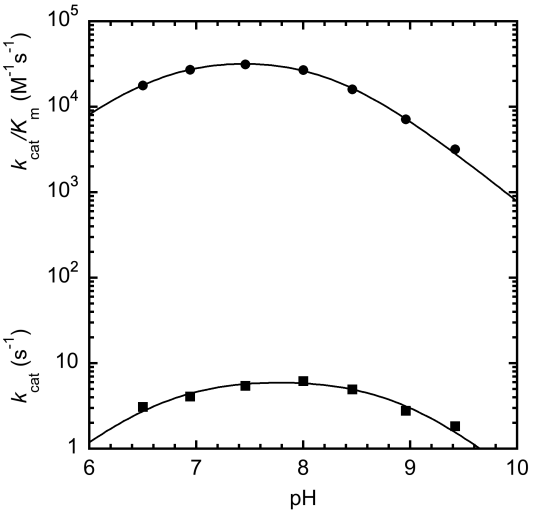

Figure 1. pH–rate profiles for MtnA-catalyzed isomerization of MTR1P. Both k_{cat} (squares) and k_{cat}/K_M (circles) profiles were fit to eq 2. Each point is the mean of triplicate measurements. Error bars are obscured by the symbols.

(8.29 ± 0.03), while that for the acidic limb remained roughly constant (~6.6) (Table 1).

Table 1. pH Dependence of Steady-State Kinetics for MtnA

Parameter	Rate constant	
	k_{cat}	k_{cat}/K_M
c^a	6.8 ± 0.5 s^{-1}	(4.1 ± 0.1) × 10^4 M^{-1} s^{-1}
pK_1	6.68 ± 0.11	6.60 ± 0.03
pK_2	8.89 ± 0.11	8.29 ± 0.03

[a] pH-independent limiting value.

These profiles indicate the presence of two catalytically relevant ionizable groups, which could correspond to the acid and base residues indicated in the proposed mechanisms. One must be cautious when attempting to assign each observed pK_a to a specific residue without additional information, as several factors can perturb the intrinsic pK_a values. Nevertheless, candidate residues can be suggested from their positioning relative to the product, as revealed by X-ray crystallography (Figure 2).[16] Notably, Asp240 makes close contacts with O-2 and O-4, which must lose and gain a proton, respectively, during isomerization (i.e., residue A in Scheme 3). Additionally, Cys160 flanks C-1 and C-2 on the same face where hydrogen transfer occurs, suggesting that it may serve as the catalytic base in one of

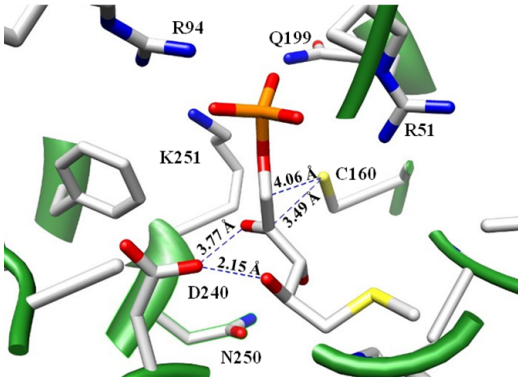

Figure 2. The active site of MtnA with MTRu1P bound (from PDB 2YVK). Dashed lines represent the distances between Cys160 and C-1 and C-2 and between Asp240 and O-2 and O-4.

mechanisms involving proton transfer (i.e., residue B in Scheme 3). Assuming these two residues do correspond to the two limbs in the pH–rate profiles, one would expect the lower pK_a (~6.6) to be associated with Asp240 and the higher pK_a (>8) to be associated with Cys160; however, such a scenario predicts these to predominantly exist in their carboxylate and thiol forms, respectively, which is the opposite of what is required for catalysis in the physiological direction. Thus, either the pK_a values are unusually swapped or MtnA uses a reverse-protonation mechanism, which is known to occur when the pK_as of the general acid and general base are within ~2 units.[24, 25] There could be other possibilities for these pK_a assignments. For example, pK_1 could be the second ionization of the substrate's phosphate ester, and pK_2 could be attributable to one of the three basic active-site residues (Arg51, Arg94, or Lys251) that bind the phosphoryl group. However, although the observed pK_a values are consistent with such assignments, they would be expected to appear only in the k_{cat}/K_m profile and not also k_{cat}.[26] This generalization is attributable to the engagement of specific hydrogen bonding between the substrate and neighboring active-site residues.

Detection and Stability of Phosphorylated Enzyme. To probe the proposed covalent mechanism, [^{32}P]MTR1P was prepared by MtnK-catalyzed phosphorylation of MTR with [γ-^{32}P]ATP, followed by HPLC purification (Figure S1). After incubating [^{32}P]MTR1P with MtnA for 30 s, the reaction mixture was separated by native polyacrylamide gel electrophoresis, transblotted onto a PVDF membrane, and exposed to a phosphor screen. ^{32}P was found to be associated with the protein band identified by Coomassie staining (Figure 3A). Likewise, denaturing SDS-PAGE also revealed comigration of radioactivity with MtnA but only under non-reducing conditions. Interestingly, when 5% (~100 mM) β-mercaptoethanol (BME) was added to the sample before electrophoresis, only trace radioactivity could be detected (Figure 3B). In fact, radioactivity was greatly diminished at concentrations of BME >1 mM, and a similar effect occurred with the phosphorus-based reducing agent tris(carboxyethyl)phosphine (TCEP) (Figure S2). These results show that MtnA becomes covalently modified by ^{32}P-labeled MTR1P and that the resulting adduct is sensitive to the presence of reducing agents, which presumably serve as nucleophiles to displace the phosphoryl group from the modified residue. Further, the radiolabeling was specific between intact MtnA and [^{32}P]MTR1P, as no labeling was detected when (1) MtnA was denatured by SDS prior to mixing (boxed lanes in Figure 3B), (2) another protein was used in place of MtnA, or (3) [γ-^{32}P]ATP was used instead of [^{32}P]MTR1P (data not shown).

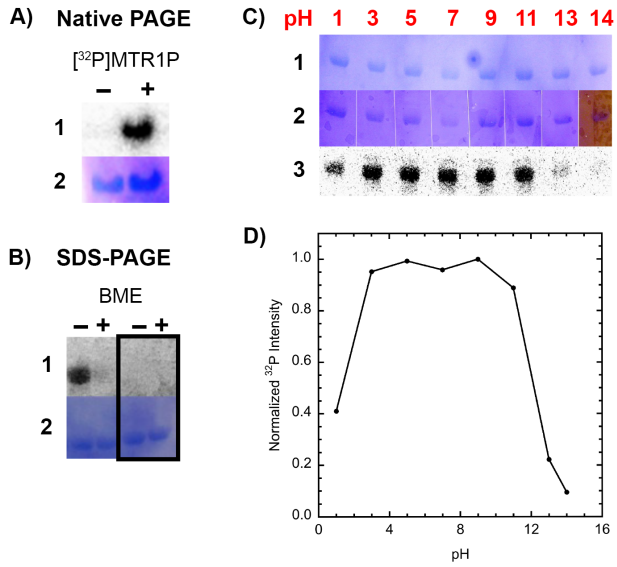

Figure 3. Detection and effect of pH on phosphorylated MtnA adduct. A) Native PAGE of MtnA incubated with (+) and without (–) [^{32}P]MTR1P. Row 1: Autoradiograph of PVDF membrane. Row 2: Coomassie-stained PVDF membrane. B) SDS-PAGE of labeled MtnA in the presence (+) and absence (–) of 5% (v/v) β-mercaptoethanol (BME). Row 1: Autoradiograph of PVDF membrane. Row 2: Coomassie-stained PVDF membrane. Lanes in box: same as other lanes but with MtnA that was denatured prior to mixing. C) Coomassie-stained PVDF membrane before (Row 1) and after (Row 2) treatment at the indicated pH for 30 min. Row 3: Autoradiograph of PVDF membrane. D) Normalized intensities of radioactive bands from row 3 in panel C as a function of pH.

The effect of pH on the stability of various phosphorylated amino acids has been studied in detail.[27] To aid in the identification of the amino acid residue that is phosphorylated by MTR1P, the effect of pH on the stability of the adduct was investigated. After SDS-PAGE and transblotting of the radiolabeled enzyme, the PVDF membrane was exposed to various pH conditions at room temperature for 30 min (Figure 3C). The results show moderate stability of the radiolabel at pH 3–11 and its lability at extreme pH (Figure 3D). At pH 1, a maximum loss of radioactivity of 60% was observed relative to that at pH 9, while at pH 13 and 14, the radioactivity decreased by 80% and 90%, respectively. The effect of pH was also tested on phosphorylated MtnA purified by size-exclusion chromatography (Figure S3). The recovered protein was incubated for 30 min at 25 °C in buffers of varying pH before being removed by ultrafiltration. Reaffirming the results from SDS-PAGE, the hydrolyzed [^{32}P]phosphate in the filtrate was greatest at high and low pH, especially at pH ≥13.

Phosphoramidate linkages common to phosphorylated lysine, arginine, and histidine residues are known to be susceptible to hydrolysis only in acid, exhibiting stability at high pH;[28] thus, the basic residues (Arg94, Arg51, and Lys251) that surround the phosphate group (Figure 2) can be excluded from consideration. Similarly, Cys160 cannot be the nucleophilic residue because phosphocysteine is also fairly stable to alkaline pH, uniquely exhibiting maximal rates of hydrolysis at pH 2–4.[29, 30] The instability of the adduct observed at high and low pH, however, is diagnostic of an acyl phosphate (mixed anhydride) formed by phosphorylation of a carboxyl group of a glutamate or aspartate residue,[31, 32] such as Asp240. Because acyl phosphates are notably susceptible to reaction with various nucleophiles, radiolabeled MtnA was subjected to reaction with varying concentrations of NH_2OH or pyridine. Accordingly, both amines led to concentration-dependent dephosphorylation of MtnA (Figure S4), consistent with an acyl phosphate.

Mechanistic Evaluation of Phosphorylated Enzyme. The fraction of the total enzyme-bound substrate that exists as a covalent adduct is a useful measure of its relative thermodynamic and kinetic stability. This was determined from mixtures of known concentrations of [^{32}P]MTR1P and excess MtnA that were separated by size-exclusion chromatography to isolate the protein from unbound substrate. For example, when 30 μM [^{32}P]MTR1P was mixed with 330 μM MtnA, the bound substrate concentration, [E•S], was calculated to be 21 μM (see Supporting Information for detailed calculations). After recovery of the protein from chromatography, the total radioactivity was counted and using the specific activity of the substrate, 3.1% of the total E•S complex was determined to have existed as a covalent adduct. This value may represent the thermodynamic limit if a step following phosphoryl transfer is rate limiting; however, if adduct formation or a step prior to it is slow, the faster subsequent steps may limit the amount of adduct that accumulates in the steady state.

To aid in identification of the rate-limiting step, the primary deuterium kinetic isotope effect (KIE) on steady-state turnover of [2-^{2}H]MTR1P was measured using the OPDA assay (Figure 4). Global

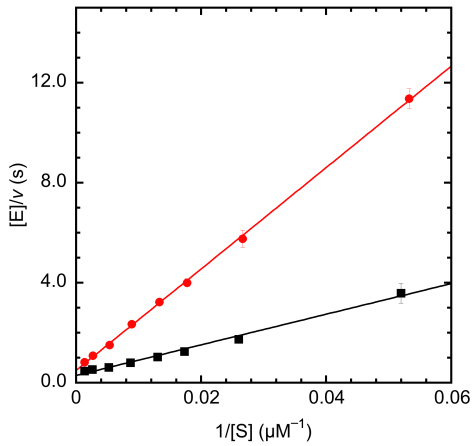

Figure 4. Primary deuterium kinetic isotope effect. Steady-state kinetics measurements were performed in parallel with MTR1P (black squares) and [2-^{2}H]MTR1P (red circles). Each point is the mean of triplicate measurements, and error bars reflect SD. This double-reciprocal plot serves to aid in visualizing the large $^D(V/K)$ (slope effect); accurate values for ^DV and $^D(V/K)$ were obtained by global fitting to eq 3 (see Figure S5).

fitting of the data revealed a modest KIE on k_{cat}, ^DV, of 1.4 ± 0.1 and a larger KIE on k_{cat}/K_M, $^D(V/K)$, of 3.9 ± 0.1. The smaller value of the former indicates that k_{cat} is sensitive to a slow step, perhaps product release, that is absent in k_{cat}/K_M. Thus, $^D(V/K)$ more effectively reflects the rate-limiting nature of the hydrogen-transfer step. Because this step must occur after phosphoryl transfer, it can be concluded that the observed 3.1% covalent adduct likely reflects the internal equilibria preceding hydrogen transfer.

If a covalent adduct is an on-pathway reactive intermediate and certain steps are slowed by mutation, one may expect the extent of labeling to be altered. Specifically, if the perturbation places the rate-limiting step at or before covalent-bond formation, the extent of radiolabeling should decrease. If the rate-limiting step occurs subsequent to adduct formation, however, radioactivity should accumulate, limited only by the internal equilibrium; such behavior was observed by Huang & Santi in active-site mutants of thymidylate

synthase.[33] In the case of MtnA, C160S and D240N were prepared to probe whether either would result in a change in radiolabeling of the enzyme. Both mutations drastically impaired catalysis, and because it was not possible to measure rates below 5 mM MTR1P, complete steady-state kinetic parameters could not be obtained. Because no significant differences in rate were observed at higher substrate concentrations, measurements at 5 mM were used to estimate k_{cat} values of 7.6×10^{-7} s^{-1} for C160S and 2.7×10^{-7} s^{-1} for D240N.

Without the knowledge of K_M for the mutants, it was not possible to calculate the fraction of covalent adduct formation as was done for the wild-type enzyme. As an alternative, the degree of labeling was assessed qualitatively by SDS-PAGE. Remarkably, both mutants behaved indistinguishably from the wild-type enzyme, demonstrating similar radioactivity intensities and pH stability (Figure 5). This

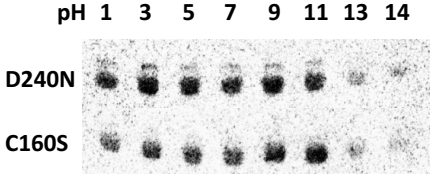

Figure 5. Detection and pH dependence of radioactive labeling of highly conserved active site mutants D240N and C160S. As with wild-type MtnA (Figure 3C), PVDF membranes were treated to the indicated pH for 30 min before autoradiography.

result is perhaps less surprising for C160S because Cys160 is believed to facilitate hydrogen transfer, which is already rate limiting for the wild-type enzyme. Asp240, on the other hand, was a candidate residue to serve as the nucleophile. Now that this role has been excluded, Asp240 is believed to serve as the Brønsted acid that protonates O-4 during ring opening. Because D240N did not exhibit reduced radiolabeling, however, it can be concluded that ring opening does not occur in concert with phosphoryl transfer from MTR1P if covalent catalysis is in fact used by MtnA.

The results from mutagenesis cast doubt on the mechanistic relevance of the phosphorylated adduct. To further assess this, the adduct recovered from size-exclusion chromatography was assayed for chemical competence by incubating it with unlabeled MTR. If MTR is capable of binding to the labeled enzyme, radiolabeled MTR1P and/or MTRu1P would be expected to be released. After extensive incubation followed by removal of the protein by ultrafiltration, no significant difference in radioactivity could be detected in the filtrate compared to a control lacking MTR. Thus, either MTR cannot effectively access the active site of the phosphorylated adduct or they are not reaction intermediates. With no other candidate nucleophiles in the vicinity of the active site, it is increasingly likely that the observed phosphorylation is an artifact and/or occurs at a remote site with no obvious functional purpose. Artifactual phosphorylation of an aspartate residue by a phosphate ester has been reported for pyrophosphatase,[34, 35] for example. It is interesting to note that oxocarbenium ion **3** (Scheme 3B or 3C) is expected to be an excellent phosphorylating agent considering the leaving group would be **4**, which is a relatively stable molecule. Considering that hydrogen transfer is slow, it is possible that occasionally **3** is intercepted by an unknown aspartate/glutamate residue and that this non-productive adduct simply reverses back to **3**. If Cys160 mediates hydrogen transfer, however, C160S should have resulted in accumulation of the adduct. Also, if Asp240 is required for ring opening, then formation of **3** and subsequent adduct formation should have been greatly diminished in D240N.

Identification of a Second Covalent Adduct by NMR. During our investigations with MtnA mutants, we questioned whether greater extents of radiolabeling could be detected if they were incubated much longer than the 30 s given before SDS-PAGE. After allowing the three variants (210 μM) to incubate with [^{32}P]MTR1P (30 μM) overnight (16 h), each protein was isolated by size-exclusion chromatography. Unexpectedly, only C160S was found to accumulate radioactivity, reaching as high as 22% of the total substrate present. Considering the K_M for this mutant was unknown, the amount of ^{32}P accumulated was measured as a function of substrate concentration, displaying saturation behavior (Figure S6). Fitting the data yielded an apparent K_M of 70 ± 30 μM and a limit of about 30% of the total enzyme possessing radioactivity. These interpretations, of course, assume that the accumulation of radioactivity is related to active-site binding and covalent reaction of [^{32}P]MTR1P. Considering the prior discussion drawing doubt about the mechanistic relevance of the short-time-scale radiolabeling, it was unclear whether this accumulation that is unique to C160S was of the same origin or resulted from a distinct reaction that may be related to authentic turnover of the substrate.

To address this concern, we performed ^{31}P-NMR spectroscopy on MTR1P in the presence of stoichiometric amounts of C160S, taking advantage of the fact that the high level of adduct accumulation permitted detection by this technique. After mixing 1.5 mM C160S with 2.0 mM MTR1P in 20 mM TEOA•HCl (pH 7.8) containing 10% D_2O, ^{31}P-NMR spectra were acquired repeatedly over the course of 14 h at 25 °C, revealing new signals at 3.8 and 8.0 ppm (Figure 6A). Note that the interval between spectra was 2 h 20 min, the time required to acquire each spectrum. By comparison to a sample treated with catalytic amounts of wild-type MtnA (Figure S7A), the upfield signal was confirmed to be MTRu1P, which only became visible after 9 h 20 min of incubation, owing to the very slow turnover number for the mutant enzyme. The broad downfield peak, on the other hand, was believed to be a protein-bound phosphorus-containing species. Peak broadening is known to occur when ligands become associated with proteins, as the resulting complexes have much longer rotational correlation times, leading to longer transverse relaxation times (T_2).[36, 37] Intriguingly, this signal first appeared after 4 h 40 min, long before the generation of MTRu1P, suggesting that it could represent an intermediate formed during isomerization.

To assess whether the signal at 8.0 ppm could be associated with a covalently bound species, the reaction mixture was subjected to size-exclusion chromatography. The ^{31}P-NMR spectrum of the recovered protein revealed the absence of MTR1P and MTRu1P, but the broad signal remained (Figure 6B). Interestingly, when a previously equilibrated mixture of MTR1P and MTRu1P, prepared by incubation with a small amount of wild-type MtnA followed by removal by ultrafiltration, was incubated with C160S, the signal at 8.0 ppm appeared in the first spectrum (Figure 6C). This result led us to hypothesize that the new signal was the result of an adduct formed between C160S and MTRu1P.

To verify if the adduct is unique to C160S, the equilibrated substrate–product mixture was also incubated with wild-type MtnA, D240N, and C160A. Interestingly, in the presence of a high concentration of the wild-type enzyme for 1 h, the signals of MTR1P and MTRu1P were reduced, while a new signal appeared at ~2.5 ppm (Figure S7B). The new peak was identified as phosphate by spiking the sample with an authentic standard. Suspecting that this could have been the result of phosphatase contamination, we additionally purified MtnA by size-exclusion chromatography and included EDTA in the buffer, but dephosphorylation persisted. Considering

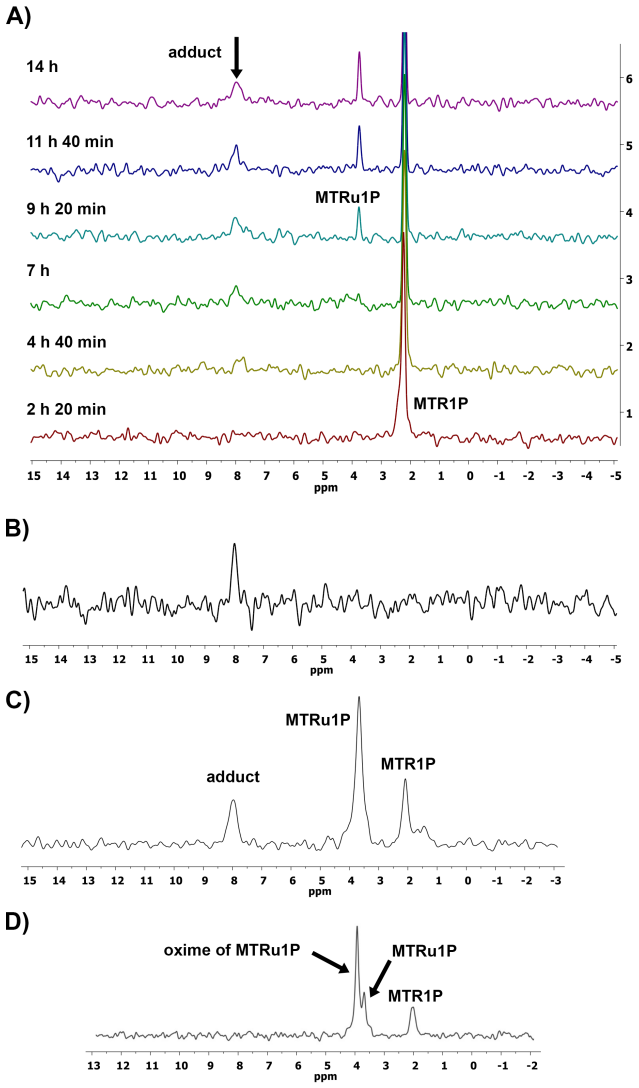

Figure 6. ^{31}P-NMR spectra of mixtures of MTR1P and/or MTRu1P and C160S. Each spectrum is the result from the accumulation of 4096 scans. A 20-Hz exponential line broadening functon was used to improve signal-to-noise of the broad peaks. A) Stacked spectra acquired successively for a sample containing 1.5 mM C160S and 2 mM MTR1P in 20 mM TEOA-HCl (pH 7.8) in 10% D_2O. The broad peak at 8.0 ppm that slowly forms prior to appearance of the product at 3.8 ppm is attributed to a covalent adduct. B) ^{31}P-NMR spectrum obtained after size-exclusion chromatography of the mixture in A after 14 h. C) ^{31}P-NMR spectrum acquired immediately after adding C160S to an equilibrated mixture of MTR1P and MTRu1P. D) ^{31}P-NMR spectrum of the sample in C after reaction with 350 mM NH_2OH.

that this activity was absent in samples with other variants, these results suggest that MtnA may occasionally catalyze a hydrolytic side reaction; this dephosphorylation is the subject of future investigations. Despite this unexpected side reaction, no ^{31}P signal associated with an adduct was detected, and passage of the sample through a size-exclusion column yielded no enzyme-bound signals. D240N failed to generate any new ^{31}P signals (data not shown), but C160A led to the appearance of a peak at 6.4 ppm (Figure S7C); however, unlike with C160S, this peak did not remain after size-exclusion purification (Figure S7D), suggesting it may have been associated with a non-covalent binary complex.

Attempts were made to intercept the adduct with nucleophilic agents. Because of the susceptibility of the radiolabeled enzyme to high concentrations of NH_2OH, the C160S adduct was similarly treated, resulting in the disappearance of the adduct and the formation of an oxime derivative of MTRu1P (Figure 6D). Because of (1) the absence of inorganic phosphate as a product, which would have been released if the enzyme were phosphorylated, (2) the fact that the oxime is the only new phosphorus-containing species, and (3) the fact that the adduct appears in the first spectrum after mixing C160S with MTRu1P, it is likely that the adduct is a reversible covalently bound form of the product, presumably via its carbonyl. Considering the proximity of Lys251 to the ligand in the active site, we first speculated that it could form a Schiff base with the ketone. Our attempt to trap the adduct by reduction with $NaCNBH_3$, however, instead resulted in the partial disappearance of the adduct peak and a corresponding appearance of a peak consistent with the product (Figure S8), which eventually became reduced to an alcohol, confirmed by direct reduction of MTRu1P with $NaCNBH_3$ in the absence of enzyme. Thus, the adduct is not a Schiff base. It is apparent that NH_2OH and $NaCNBH_3$ react with free MTRu1P and by Le Chatelier's principle, continue to react with the MTRu1P that is released from the adduct.

To verify unequivocally that MTRu1P reacts with C160S via its carbonyl, ^{13}C NMR was performed using ^{13}C-labeled substrate and product. First, separate equilibrium mixtures of [1-^{13}C]MTR1P and -MTRu1P, [2-^{13}C]MTR1P and -MTRu1P, and [1,2-$^{13}C_2$]MTR1P and -MTRu1P were prepared using catalytic amounts of wild-type MtnA. A representative ^{13}C-NMR spectrum of the dilabeled mixture is given in Figure 7A. Next, after removal of the wild-type enzyme,

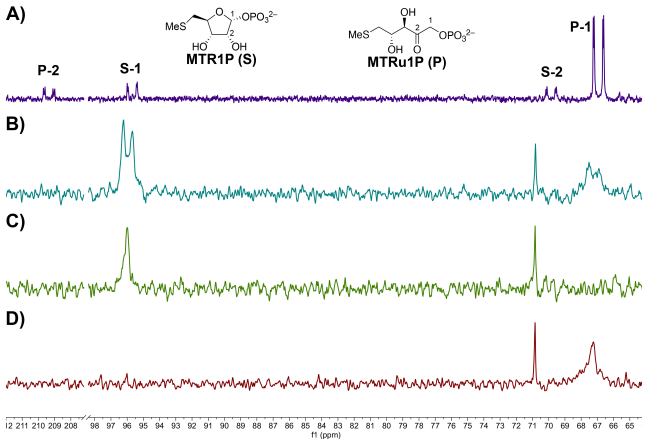

Figure 7. ^{13}C-NMR spectra of ^{13}C-labeled MTR1P and MTRu1P before and after treatment with C160S. A) Mixture of [1,2-$^{13}C_2$]MTR1P (S) and [1,2-$^{13}C_2$]MTRu1P (P) in the absence of C160S. The signals from C-1 and C-2 of the respective species have been labeled. The lower three panels represent isolated enzyme adducts prepared by mixing C160S with B) [1,2-$^{13}C_2$]MTRu1P, C) [2-^{13}C]MTRu1P, and D) [1-^{13}C]MTRu1P. ^{31}P coupling is not visible in B–D due application of an exponential line-broadening function (5 Hz) to improve signal-to-noise ratios. The singlet at 70.9 ppm is from glycerol, which was present in the enzyme's storage buffer.

each mixture was incubated with C160S, and the protein was isolated by size-exclusion chromatography. The presence of the adduct in each sample was confirmed by ^{31}P NMR. The ^{13}C-NMR spectrum of the dilabeled sample reveals signals at 96.0 and 67.5 ppm, each

exhibiting ^{13}C–^{13}C splitting (Figure 7B). To confirm that these peaks were not artifactual, the same experiment was carried out with [2-^{13}C]- (Figure 7C) and [1-^{13}C]MTRu1P (Figure 7D) separately, identifying the signals at 96.0 and 67.5 ppm, respectively. Because the covalent enzyme adduct was formed only with C160S and not C160A and based on the ^{13}C chemical shifts of the adduct peaks, we conclude that the adduct is a hemiketal resulting from reaction between Ser160 and the carbonyl group of MTRu1P (Scheme 5, X = O). Aldehydes are known inhibitors of serine proteases and are proposed to form hemiacetal intermediates.[38] ^{13}C-NMR chemical shifts at 95.5 ppm have been reported for such hemiacetal and hemiketal adducts with chymotrypsin, which is strikingly similar to the chemical shift at 96.0 ppm observed here.[39]

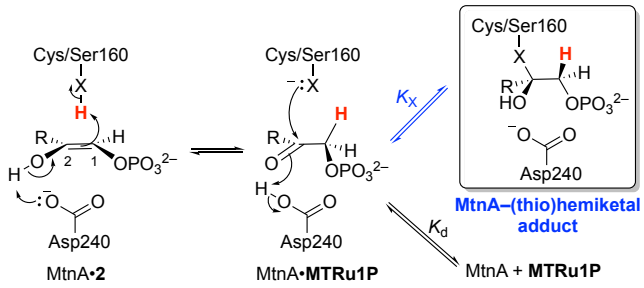

Scheme 5. Proposed mechanism for formation of C160S–hemiketal (X = O) or MtnA–thiohemiketal (X = S), where $K_O >> K_S$. K_d = dissociation constant for MTRu1P; **2** = *cis*-enediol intermediate; R = –CH(OH)CH(OH)CH$_2$SCH$_3$.

We interpret the accumulation of the hemiketal with C160S as indirect evidence for a mechanism involving proton transfer mediated by Cys160 (i.e., Scheme 3A or 3B). First, recall that turnover of C160S was greatly reduced, which can be explained by replacement by a group with a much higher pK_a, which would therefore be present as the conjugate base in minute concentrations at pH 7.5–8.0, impairing *cis*-enediol (**2**) formation. Second, after transferring the proton back from Ser160 to C-1 of the *cis*-enediol, regeneration of the relatively unstable alkoxide in direct proximity to one face of the carbonyl, nucleophilic attack to form the hemiketal immediately occurs to intercept the product faster than it can dissociate (Scheme 5), consistent with the order of appearance of the signals in the ^{31}P-NMR experiment.

In solution, the equilibrium and corresponding equilibrium constant (K_{ROH}) for hemiketal (HK) formation from a ketone (R_2CO) and an alcohol (ROH) are given by eq 4 and 5.

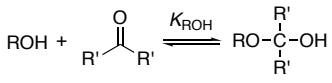

(4)

$$K_{ROH} = [HK]/([ROH][R'_2CO]) \quad (5)$$

Although the magnitude of K_{ROH} is typically small (e.g., 2.2×10^{-4} for methanol and acetone),[40] the relevant reaction for discussion involves an alkoxide (RO^-) and a proton instead of an alcohol, as in eq 6 and 7.

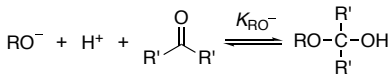

(6)

$$K_{RO^-} = [HK]/([RO^-][H^+][R'_2CO]) = K_{ROH}/K_{a,ROH} \quad (7)$$

With $K_{a,ROH} \sim 10^{-16}$, it's clear that hemiketal formation from an alkoxide and a proton is tremendously favorable. In a buffered solution near neutral pH, this reaction is of course negligible due to the very low concentrations of the alkoxide and proton, but in the confines of the enzyme's active site where all three reactants are positioned appropriately, hemiketal formation would be highly favorable. Why, then, does a thiohemiketal (X = S) not similarly accumulate in the wild-type enzyme? The thermodynamics of thiohemiketal formation has been discussed by Jencks, who concluded that carbonyls generally react more favorably with thiols than with alcohols (i.e., $K_{RSH} > K_{ROH}$).[41,42] This increase, however, is more than offset by the much higher $K_{a,RSH} \sim 10^{-10}$ expected for a cysteine thiol. Thus, by comparison of eq 7 for RO^- and the equivalent for RS^-, hemiketal formation from an alkoxide and a proton is expected to be much more favorable than thiohemiketal formation from a thiolate and a proton. Consequently, one may predict a similar effect on the on-enzyme equilibrium. i.e., $K_S << K_O$ (Scheme 5). Thus, any adduct that might form in the active-site of the wild-type enzyme does not accumulate and the enzyme–product complex partitions favorably towards product release (K_d).

Conclusion

In this investigation, evidence was provided for the formation of two covalent adducts between MtnA and its substrate, MTR1P. The first of these formed immediately after mixing and was found to be stable to SDS-PAGE and gel-filtration chromatography but sensitive to extreme pH and nucleophilic agents, hallmarks of an acyl phosphate formed by phosphoryl transfer from the substrate to an aspartate or glutamate residue. However, mutation of two critical active-site residues, Asp240 and Cys160, had no effect on the degree of protein phosphorylation. Together with the failure of the isolated adduct to demonstrate chemical competence, these observations led us to conclude that the adduct is not related to the catalytic activity of the isomerase and that a covalent mechanism is unlikely. To our surprise, we discovered a second covalent adduct when C160S was incubated with MTR1P for extended periods. ^{31}P and ^{13}C NMR confirmed the formation of a stable hemiketal between Ser160 and the carbonyl of the product, MTRu1P. The catalytic impairment and adduct accumulation uniquely associated with this mutant is attributed to the increased pK_a of this residue, providing indirect support for a mechanism that utilizes Cys160 as an acid/base for transferring the proton from C-2 to C-1 during catalysis. Additional kinetics studies to resolve the chemical mechanism are underway.

ASSOCIATED CONTENT

Supporting Information

The Supporting Information is available free of charge at https://pubs.acs.org.

HPLC purification of [^{32}P]MTR1P, effect of nucleophiles and pH on MtnA phosphoryl adduct, Michaelis–Menten plots for 2-^{2}H KIE, calculation of percentage ^{32}P labeling of MtnA and C160S, ^{31}P-NMR spectra of wild-type MtnA, C160S, and C160A with MTRu1P and of C160S after treatment with NaBH$_3$CN.

Accession Codes

B. subtilis MtnA, UniProtKB O31662 (MTNA_BACSU); *B. subtilis* MtnB, UniProtKB O31668 (MTNB_BACSU); *B. subtilis* MtnK, UniProtKB O31663 (MTNK_BACSU).

AUTHOR INFORMATION

Corresponding Author

* Phone: 1-716-645-4249. E-mail: amurkin@buffalo.edu

Present Addresses

†V. M. Veeramachineni: Laboratory of Bacterial Polysaccharides, Center for Biologics Evaluation & Research, U.S. Food & Drug Administration, Silver Spring, Maryland 20993, United States.

Funding Sources

This document was supported by NSF Award CHE1808449 and CAREER Award CHE1255136 (A.S.M.).

Notes

The authors declare no competing financial interest.

REFERENCES

1. Auger, S.; Danchin, A.; Martin-Verstraete, I., Global expression profile of Bacillus subtilis grown in the presence of sulfate or methionine. *J. Bacteriol.* **2002,** *184* (18), 5179-5186.

2. Kertesz, M. A., Riding the sulfur cycle - metabolism of sulfonates and sulfate esters in Gram-negative bacteria. *FEMS Microbiol. Rev.* **2000,** *24* (2), 135-175.

3. Leustek, T.; Saito, K., Sulfate transport and assimilation in plants. *Plant Physiol.* **1999,** *120* (3), 637-643.

4. Sekowska, A.; Kung, H.-F.; Danchin, A., Sulfur metabolism in Escherichia coli and related bacteria: facts and fiction. *J. Mol. Microbiol. Biotechnol.* **2000,** *2* (2), 145-177.

5. Ashida, H.; Saito, Y.; Kojima, C.; Kobayashi, K.; Ogasawara, N.; Yokota, A., A Functional Link Between RuBisCO-like Protein of Bacillus and Photosynthetic RuBisCO. *Science* **2003,** *302* (5643), 286-290.

6. Sigman, D. S.; Boyer, P. D.; Editors, *The Enzymes, Vol. 19: Mechanisms of Catalysis. 3rd Ed*. Academic Press, Inc.: 1990; p 459 pp.

7. Zimmerman, J., Enzymatic Reaction Mechanisms by Perry A. Frey and Adrian D. Hegeman. *Biochem. Mol. Biol. Educ.* **2008,** *36* (3), 247-248.

8. Raines, R. T.; Knowles, J. R., The mechanistic pathway of a mutant triosephosphate isomerase. *Ann. N. Y. Acad. Sci.* **1986,** *471* (Int. Symp. Bioorg. Chem., 1985), 266-271.

9. Richard, J. P., Acid-base catalysis of the elimination and isomerization reactions of triose phosphates. *J. Am. Chem. Soc.* **1984,** *106* (17), 4926-4936.

10. Boyer, P. D.; Editor, *The Enzymes, Vol. 2: Kinetics and Mechanism. 3rd ed*. Academic: 1970; p 599 pp.

11. Nagorski, R. W.; Richard, J. P., Mechanistic Imperatives for Enzymic Catalysis of Aldose-Ketose Isomerization: Isomerization of Glyceraldehyde in Weakly Alkaline Aqueous Solution Occurs with Intramolecular Transfer of a Hydride Ion. *J. Am. Chem. Soc.* **1996,** *118* (31), 7432-7433.

12. Allen, K. N.; Lavie, A.; Farber, G. K.; Glasfeld, A.; Petsko, G. A.; Ringe, D., Isotopic Exchange plus Substrate and Inhibition Kinetics of D-Xylose Isomerase Do Not Support a Proton-Transfer Mechanism. *Biochemistry* **1994,** *33* (6), 1481-1487.

13. Zheng, Y. J.; Merz, K. M., Jr.; Farber, G. K., Theoretical examination of the mechanism of aldose-ketose isomerization. *Protein Eng.* **1993,** *6* (5), 479-484.

14. Saito, Y.; Ashida, H.; Kojima, C.; Tamura, H.; Matsumura, H.; Kai, Y.; Yokota, A., Enzymatic characterization of 5-methylthioribose 1-phosphate isomerase from Bacillus subtilis. *Biosci., Biotechnol., Biochem.* **2007,** *71* (8), 2021-2028.

15. Imker, H. J.; Fedorov, A. A.; Fedorov, E. V.; Almo, S. C.; Gerlt, J. A., Mechanistic Diversity in the RuBisCO Superfamily: The "Enolase" in the Methionine Salvage Pathway in Geobacillus kaustophilus. *Biochemistry* **2007,** *46* (13), 4077-4089.

16. Tamura, H.; Saito, Y.; Ashida, H.; Inoue, T.; Kai, Y.; Yokota, A.; Matsumura, H., Crystal structure of 5-methylthioribose 1-phosphate isomerase product complex from Bacillus subtilis: implications for catalytic mechanism. *Protein Sci.* **2008,** *17* (1), 126-135.

17. Kabuyama, Y.; Litman, E. S.; Templeton, P. D.; Metzner, S. I.; Witze, E. S.; Argast, G. M.; Langer, S. J.; Polvinen, K.; Shellman, Y.; Chan, D.; Shabb, J. B.; Fitzpatrick, J. E.; Resing, K. A.; Sousa, M. C.; Ahn, N. G., A mediator of Rho-dependent invasion moonlights as a methionine salvage enzyme. *Mol. Cell. Proteomics* **2009,** *8* (10), 2308-2320.

18. Wilkins, M. R.; Gasteiger, E.; Bairoch, A.; Sanchez, J.-C.; Williams, K. L.; Appel, R. D.; Hochstrasser, D. F., Protein identification and analysis tools in the ExPASy server. *Methods Mol. Biol. (Totowa, N. J.)* **1999,** *112* (2-D Proteome Analysis Protocols), 531-552.

19. Myers, R. W.; Abeles, R. H., Conversion of 5-S-methyl-5-thio-D-ribose to methionine in Klebsiella pneumoniae. Stable isotope incorporation studies of the terminal enzymic reactions in the pathway. *J. Biol. Chem.* **1990,** *265* (28), 16913-16921.

20. Overend, W. G.; Parker, L. F. J., Synthesis of 5-thiomethylribose. *Nature* **1951,** *167*, 527-528.

21. Baykov, A. A.; Evtushenko, O. A.; Avaeva, S. M., A malachite green procedure for orthophosphate determination and its use in alkaline phosphatase-based enzyme immunoassay. *Anal. Biochem.* **1988,** *171* (2), 266-270.

22. Amyes, T. L.; Richard, J. P., Enzymatic Catalysis of Proton Transfer at Carbon: Activation of Triosephosphate Isomerase by Phosphite Dianion. *Biochemistry* **2007,** *46* (19), 5841-5854.

23. Kholodar, S. A.; Tombline, G.; Liu, J.; Tan, Z.; Allen, C. L.; Gulick, A. M.; Murkin, A. S., Alteration of the flexible loop in 1-deoxy-D-xylulose-5-phosphate reductoisomerase boosts enthalpy-driven inhibition by fosmidomycin. *Biochemistry* **2014,** *53* (21), 3423-3431.

24. Sims, P. A.; Larsen, T. M.; Poyner, R. R.; Cleland, W. W.; Reed, G. H., Reverse protonation is the key to general acid-base catalysis in enolase. *Biochemistry* **2003,** *42* (27), 8298-8306.

25. Cleland, W. W., Determining the chemical mechanisms of enzyme-catalyzed reactions by kinetic studies. *Adv. Enzymol. Relat. Areas Mol. Biol.* **1977,** *45*, 273-387.

26. Cook, P. F.; Cleland, W. W., *Enzyme Kinetics and Mechanism*. Garland Science: 2007.

27. Marmelstein, A. M.; Moreno, J.; Fiedler, D., Chemical Approaches to Studying Labile Amino Acid Phosphorylation. *Top Curr Chem (Cham)* **2017,** *375* (2), 22.

28. Besant, P. G.; Attwood, P. V.; Piggott, M. J., Focus on phosphoarginine and phospholysine. *Curr Protein Pept Sci* **2009,** *10* (6), 536-550.

29. Guan, K. L.; Dixon, J. E., Evidence for protein-tyrosine-phosphatase catalysis proceeding via a cysteine-phosphate intermediate. *J. Biol. Chem.* **1991,** *266* (26), 17026-17030.

30. Herr, E. B., Jr.; Koshland, D. E., Jr., Acid and base catalysis in a non-enzymic transfer reaction; a possible enzyme model. *Biochim Biophys Acta* **1957,** *25* (1), 219-220.

31. Anthony, R. S.; Spector, L. B., Phosphorylated acetate kinase. Its isolation and reactivity. *J. Biol. Chem.* **1972,** *247* (7), 12120-12125.

32. Koshland, D. E., Effect of Catalysts on the Hydrolysis of Acetyl Phosphate. Nucleophilic Displacement Mechanisms in Enzymatic Reactions1. *Journal of the American Chemical Society* **1952,** *74* (9), 2286-2292.

33. Huang, W.; Santi, D. V., Isolation of a covalent steady-state intermediate in glutamate 60 mutants of thymidylate synthase. *J. Biol. Chem.* **1994,** *269* (50), 31327-31329.

34. Si, Y.; Wang, X.; Yang, G.; Yang, T.; Li, Y.; Ayala, G. J.; Li, X.; Wang, H.; Su, J., Crystal Structures of Pyrophosphatase from Acinetobacter baumannii: Snapshots of Pyrophosphate Binding and

Identification of a Phosphorylated Enzyme Intermediate. *Int J Mol Sci* **2019,** *20* (18), 4394.

35. Grigor'eva, O. V.; Mit'kevich, V. A.; Skliankina, V. A.; Avaeva, S. M., Inhibition of inorganic pyrophosphatase from Escherichia coli with inorganic phosphate. *Bioorg. Khim* **2001,** *27* (1), 32-39.

36. Fossel, E. T.; Post, R. L.; O'Hara, D. S.; Smith, T. W., Phosphorus-31 nuclear magnetic resonance of phosphoenzymes of sodium- and potassium-activated and of calcium-activated adenosinetriphosphatase. *Biochemistry* **1981,** *20* (25), 7215-7219.

37. Matheis, G.; Whitaker, J. R., 31P NMR chemical shifts of phosphate covalently bound to proteins. *Int. J. Biochem.* **1984,** *16* (8), 867-873.

38. Thompson, R. C., Use of peptide aldehydes to generate transition-state analogs of elastase. *Biochemistry* **1973,** *12* (1), 47-51.

39. Cleary, J. A.; Doherty, W.; Evans, P.; Malthouse, J. P. G., Hemiacetal stabilization in a chymotrypsin inhibitor complex and the reactivity of the hydroxyl group of the catalytic serine residue of chymotrypsin. *Biochimica et Biophysica Acta (BBA) - Proteins and Proteomics* **2014,** *1844* (6), 1119-1127.

40. Guthrie, J. P., Carbonyl Addition-Reactions - Factors Affecting Hydrate-Hemiacetal and Hemiacetal-Acetal Equilibrium-Constants. *Can J Chem* **1975,** *53* (6), 898-906.

41. Jencks, W. P., Mechanism and Catalysis of Simple Carbonyl Group Reactions. *Prog Phys Org Chem* **1964,** *2*, 63-128.

42. Lienhard, G. E.; Jencks, W. P., Thiol addition to the carbonyl group. Equilibria and kinetics. *J. Am. Chem. Soc.* **1966,** *88* (17), 3982-3994.

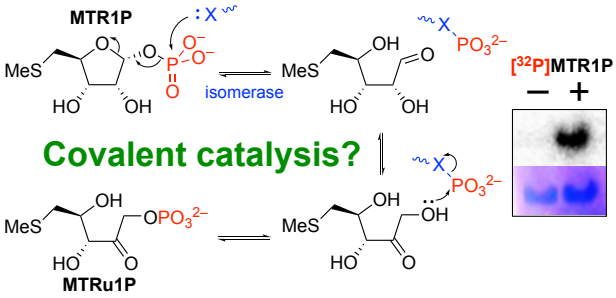

For Table of Contents use only